

Electronic Supplementary Information

Tuning antimicrobial properties of biomimetic nanopatterned surfaces

Martyna Michalska,^a Francesca Gambacorta,^a Ralu Divan,^b Igor S. Aranson,^{c,d} Andrey Sokolov,^c Philippe Noirot^a & Philip D. Laible,^{*a}

^a Biosciences Division, Argonne National Laboratory, Argonne, IL 60439, USA

E-mail: laible@anl.gov

^b Center for Nanoscale Materials, Argonne National Laboratory, Argonne, IL 60439, USA

^c Materials Science Division, Argonne National Laboratory, Argonne, IL 60439, USA

^d Department of Biomedical Engineering, Pennsylvania State University, University Park, PA 16802

Nanopillar densities were measured as number of nanopillars per surface area using SEM images, top view mode. Lengths (L) were measured using SEM images, cross section view. Having knowns such as pillar density/surface, length and base radius (r), we could further calculate Wenzel roughness defined in Wenzel model as a ratio of actual, microscopic area (etched area) to apparent area, the projection of the microscopic area on the plane (smooth area).

Since smooth area equals 1, therefore roughness equals etched area.

Etched area = (total area - area occupied by pillars) + area of pillars

Etched area = (1 - area occupied by pillars) + area of pillars

$$\text{area of pillars} = \frac{\text{pillar density}}{\text{cm}^2} \times (\pi r \times (r + \sqrt{l^2 + r^2})) \quad (\text{Eq. S1})$$

$$\text{area of occupied by pillars} = \frac{\text{pillar density}}{\text{cm}^2} \times (\pi r^2) \quad (\text{Eq. S2})$$

Bactericidal efficiency (BE) is determined based on the percentage of bacteria recovered from bSi *versus* control surface. The following equation was used for calculation:

$$\text{bacterial efficiency} = 100 - \left(\frac{\text{\#colonies after incubation on bSi}}{\text{\#colonies after incubation on Si}} \times 100 \right) \quad (\text{Eq. S3})$$

Table S1. Morphological and physical features of strains used in this study.

Characteristic	<i>E. coli</i>	<i>P. fluorescens</i>	<i>R. sphaeroides</i>	<i>R. capsulatus</i>	<i>B. subtilis</i>
Strain	DH5α	SBW25	ΔrshI	U43	NCBI 3610
Cell shape	rod	rod	rod	rod	rod
Cell size: diameter (μm)	0.5 - 1	0.5 - 0.6	0.6 - 1	0.5 - 1.2	1
length (μm)	1.7 - 2.5 ¹	1.5 - 2 ²	1.5 - 2.5 ³	2 - 2.5 ⁴	3-5 ⁵
Motility ^{4,6}	Peritrichously flagellated	Multiple polar flagella	Single polar flagellum	Single lateral flagellum	Peritrichously flagellated
Cell rigidity:					
Viscoelastic parameters k ₁ and k ₂ (Nm ⁻¹) ⁷	0.056 and 0.54	0.044 and 0.81*	---	---	---
Longitudinal ⁸ Young's modulus (MPa)	50-150	100-200*	---	---	100-200
Biofilm formation	+	+	+	+	+

*data for *P. aeruginosa*

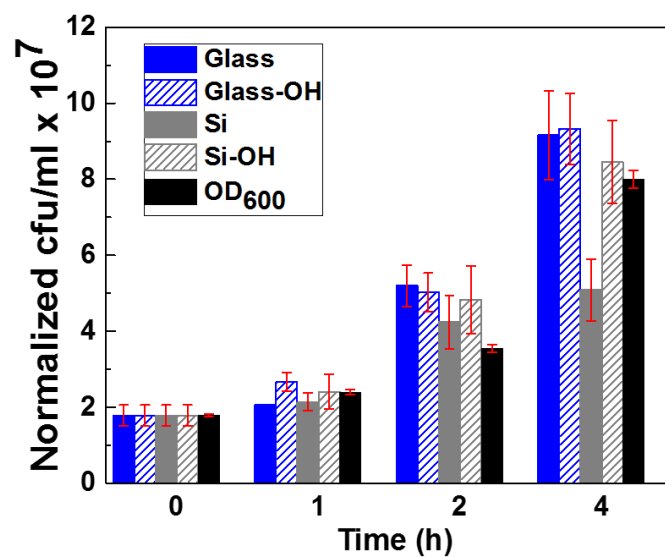


Fig. S1 Growth of *E. coli* on various control surfaces, including silicon wafers (Si), air-plasma treated silicon wafers (Si-OH), glass cover slides (glass), and air-plasma treated glass cover slides (glass-OH), versus cells in static liquid culture (prepared in microfuge tubes with turbidity measured as OD₆₀₀ values). Surface studies commenced when 20 μ l droplets (1.6×10^7 cfu/ml) were placed on the control surfaces and incubated in the humidity-controlled reaction chambers (Figure 3A) at RT.

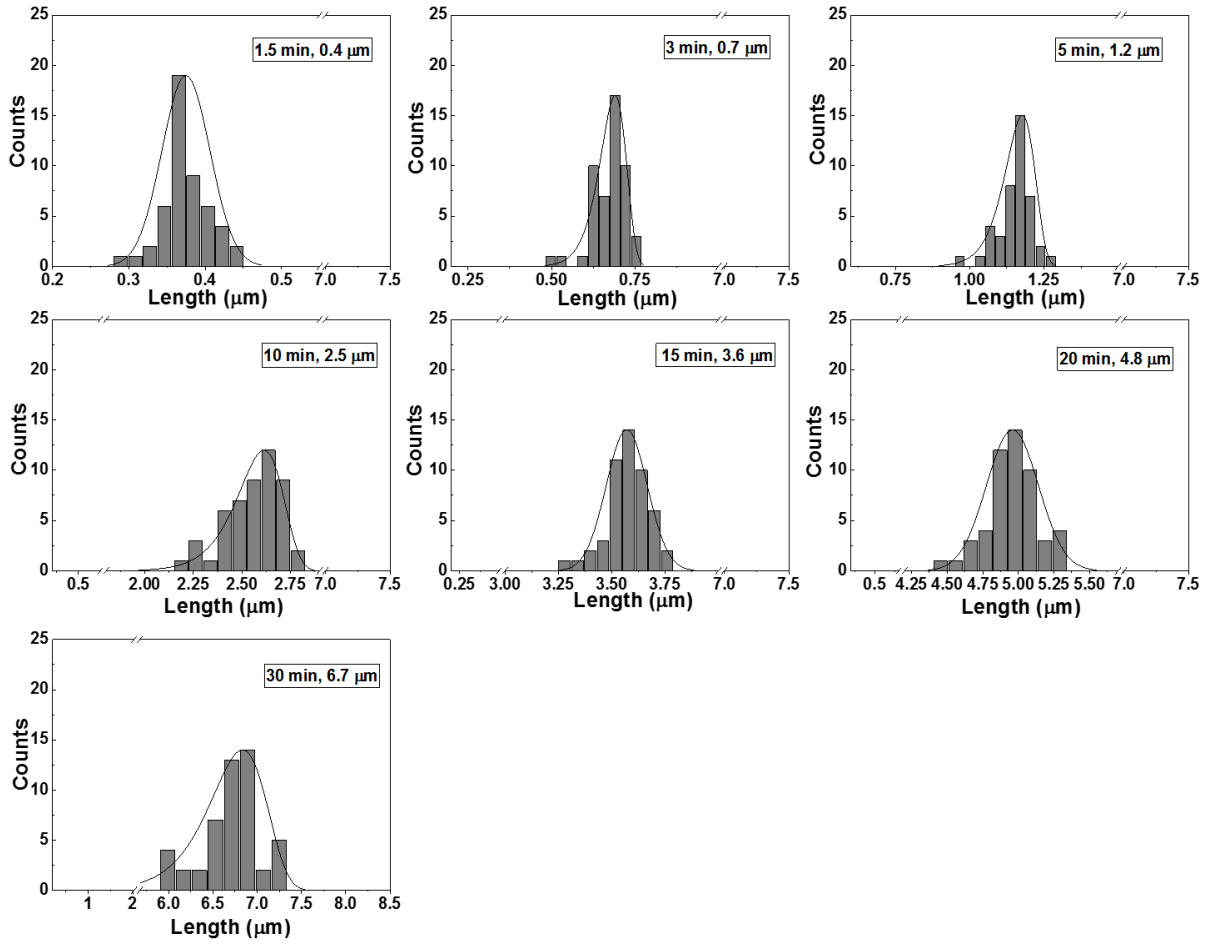


Fig. S2 Distributions of nanopillar lengths of black silicon etched for 1.5, 3, 5, 10, 15, 20 and 30 min.

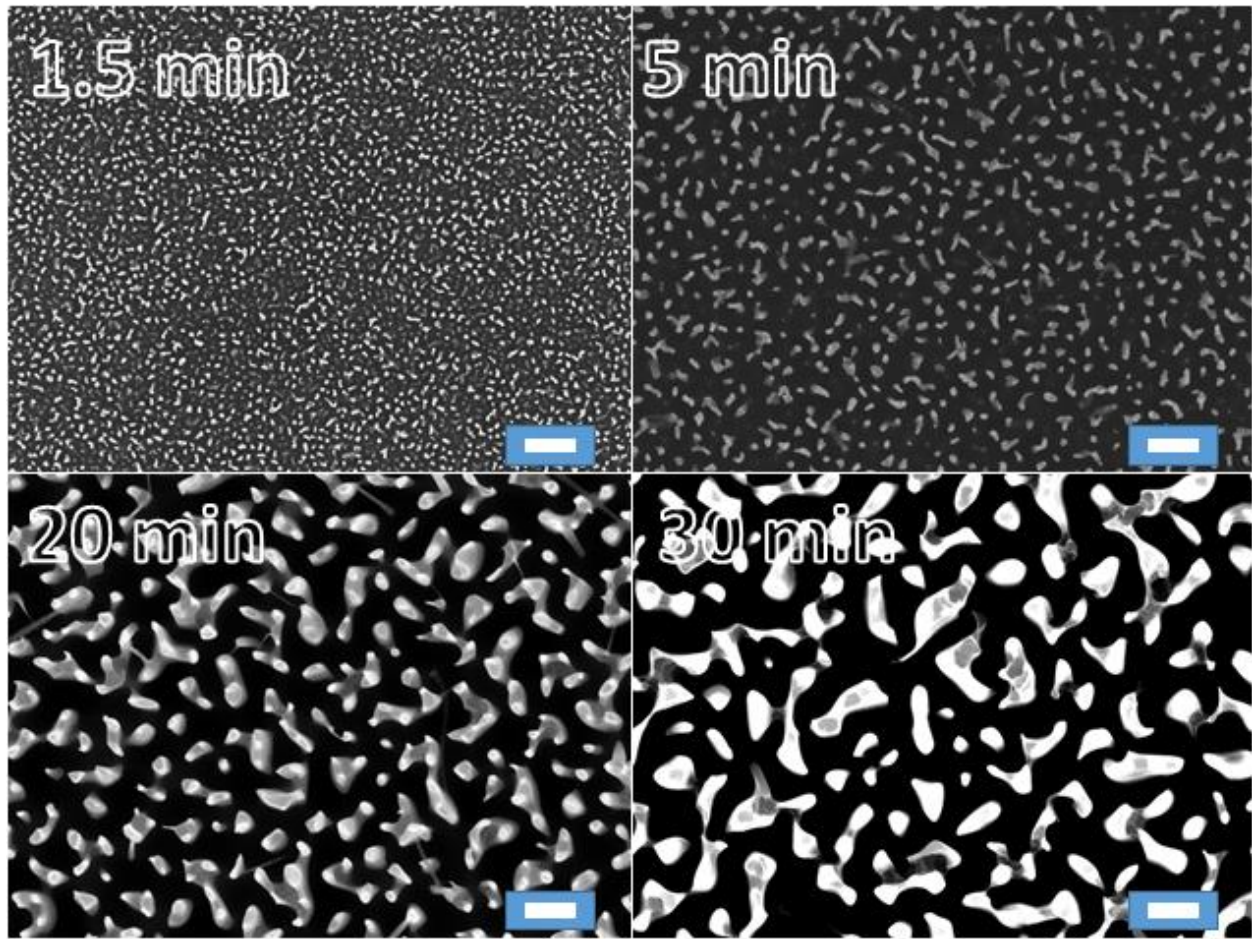


Fig. S3 SEM micrographs (top views) presenting the nanotopography of black silicon fabricated using a range of etching times: 1.5, 5, 20 and 30 min. Scale bars are preserved at 1 μm in all images.

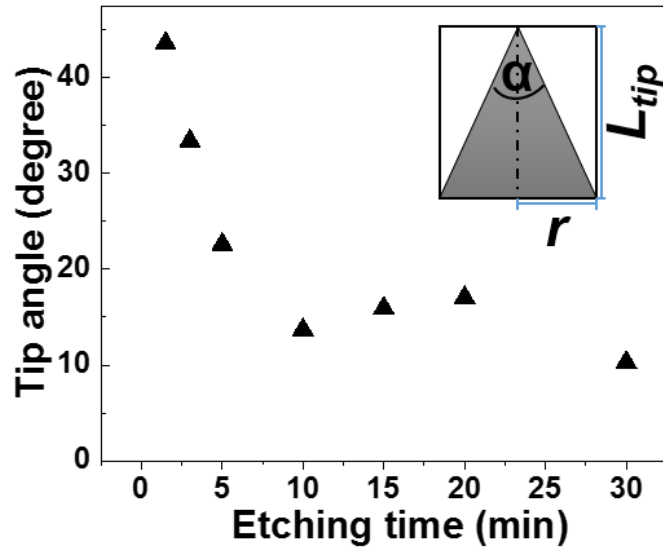


Fig. S4 The temporal evolution of the sharpness of the bSi nanopillars – as parameterized by the tip angle (α) – during the fabrication process, spanning 1.5 to 30 min. The inset schematically represents how the tip angle was calculated with the equation: $\alpha = 2 \cdot \arctan\left(\frac{r}{L_{tip}}\right)$ based upon the radius (r) and measured tip length (L_{tip}) of the nanopillars.

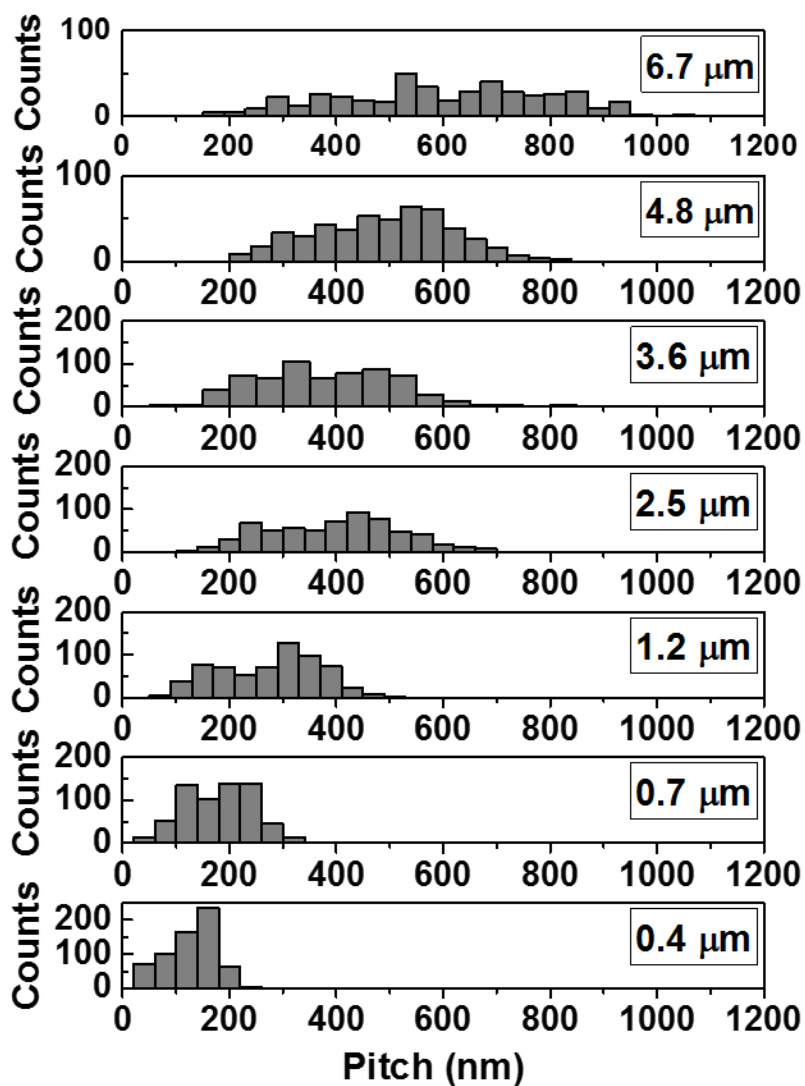


Fig. S5 Distributions of nanopillar pitches for black silicon fabricated for 1.5, 3, 5, 10, 15, 20 and 30 min (bottom to top) that correspond to nanopillar lengths of 0.4, 0.7, 1.2, 2.5, 3.6 4.8, and 6.7 μm , respectively. Pitch is the distance between two spikes at the closest proximity (pitch = spacing + base diameter) as diagrammed on Figure 2d.

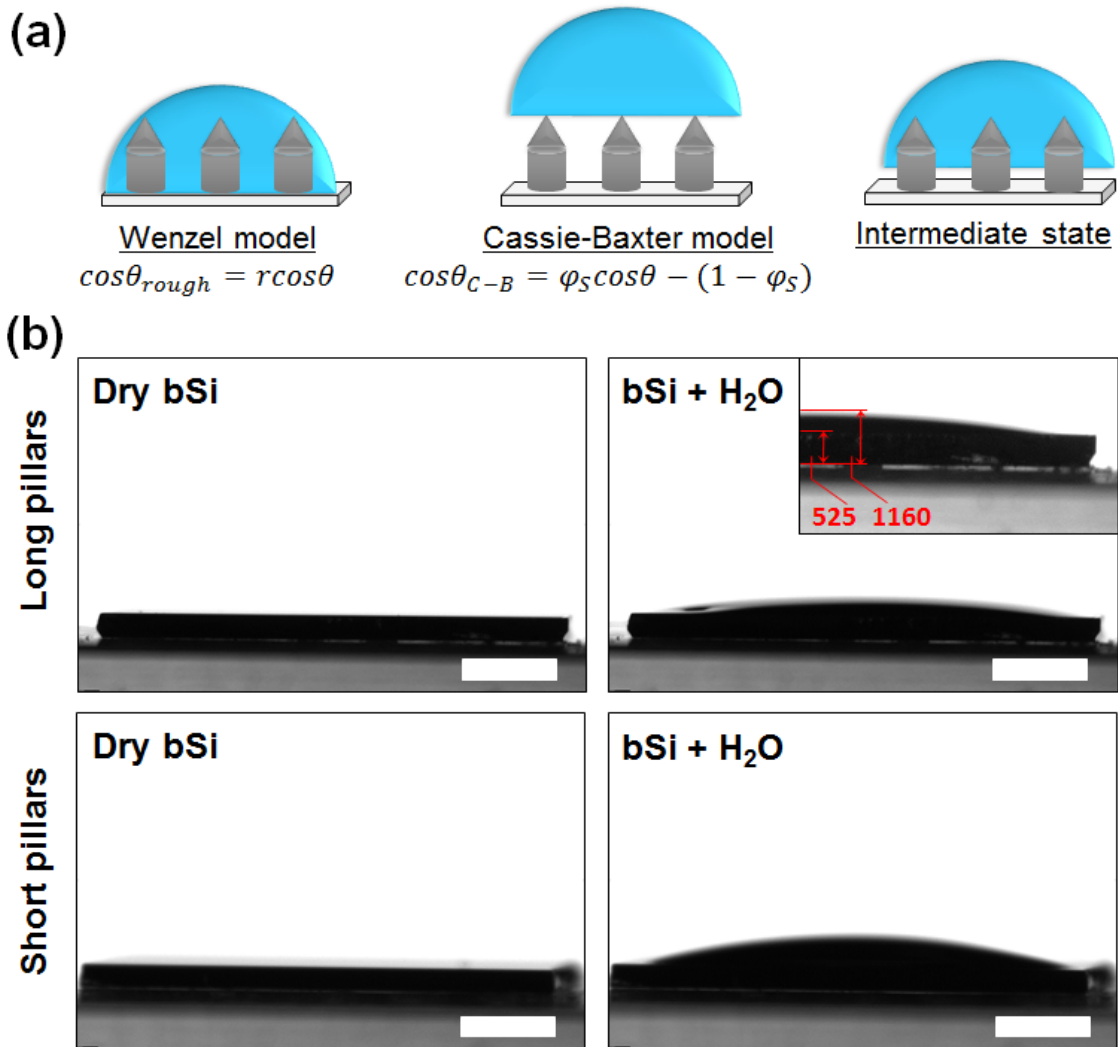


Fig. S6 (a) Graphic representation of water droplet behavior in the Wenzel model, Cassie-Baxter model, and an intermediate state. The equations describe the Wenzel model where ϑ is the Young's contact angle on the flat surface and r is roughness and the Cassie-Baxter model (C-B), where ϑ is the Young's contact angle on the flat surface and ϕ_s is the fraction of the liquid's base in contact with the solid surface.⁹ (b) Lateral images of black silicon before and after the deposition of 20 μl of H₂O. Upper and lower rows correspond to bSi with long and short pillars, respectively. Scale bars are 2 mm. The inset presents a magnified view of droplet on the superhydrophilic surface. The wafer thickness and maximum meniscus height are given in μm .

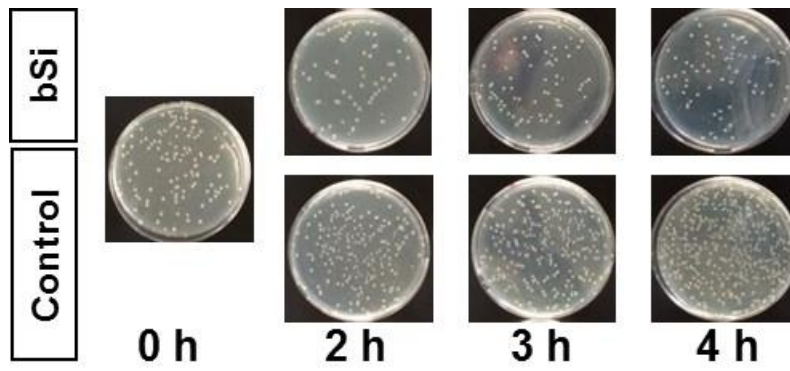


Fig. S7 Bacterial viability on black silicon surface. Colony forming units (cfu) are measured by plating *E. coli* cells exposed to etched (bSi) and smooth (control) surfaces for various times on

LB agar.

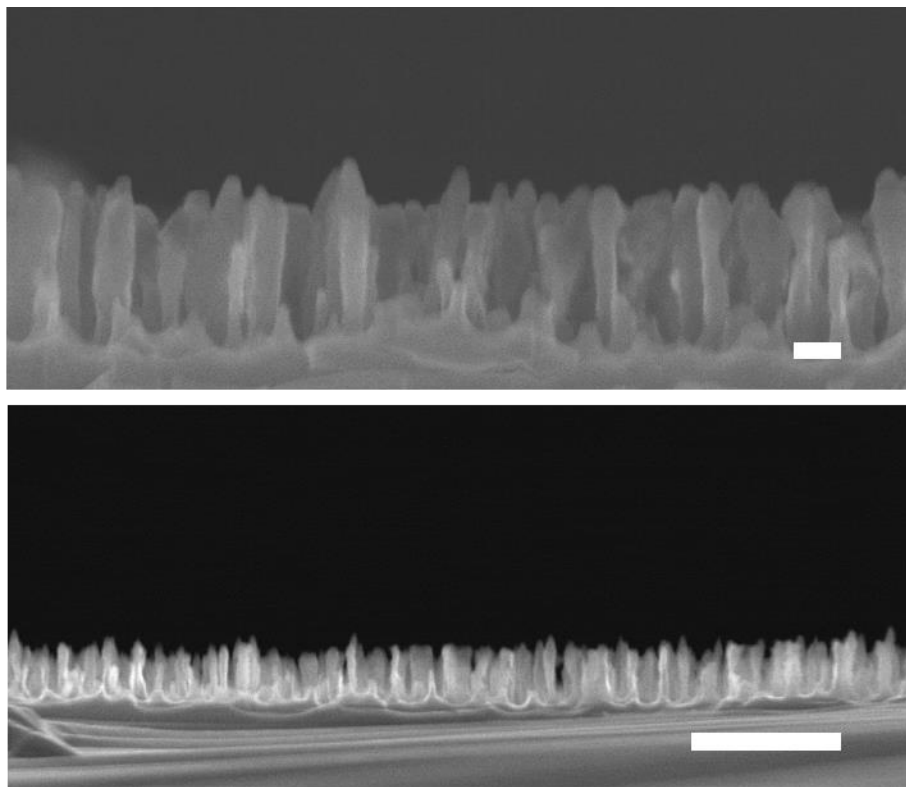


Fig. S8 SEM images of bSi etched for 1.5 min. The average nanopillar length is 390 nm (Table 1). Scale bars are 100 nm (top) and 1 μ m (bottom). These images emphasize the blunt nature of the tips of these nanopillars with tip angle (i.e., sharpness) averaging 44 $^\circ$, with many displaying onion-like features.

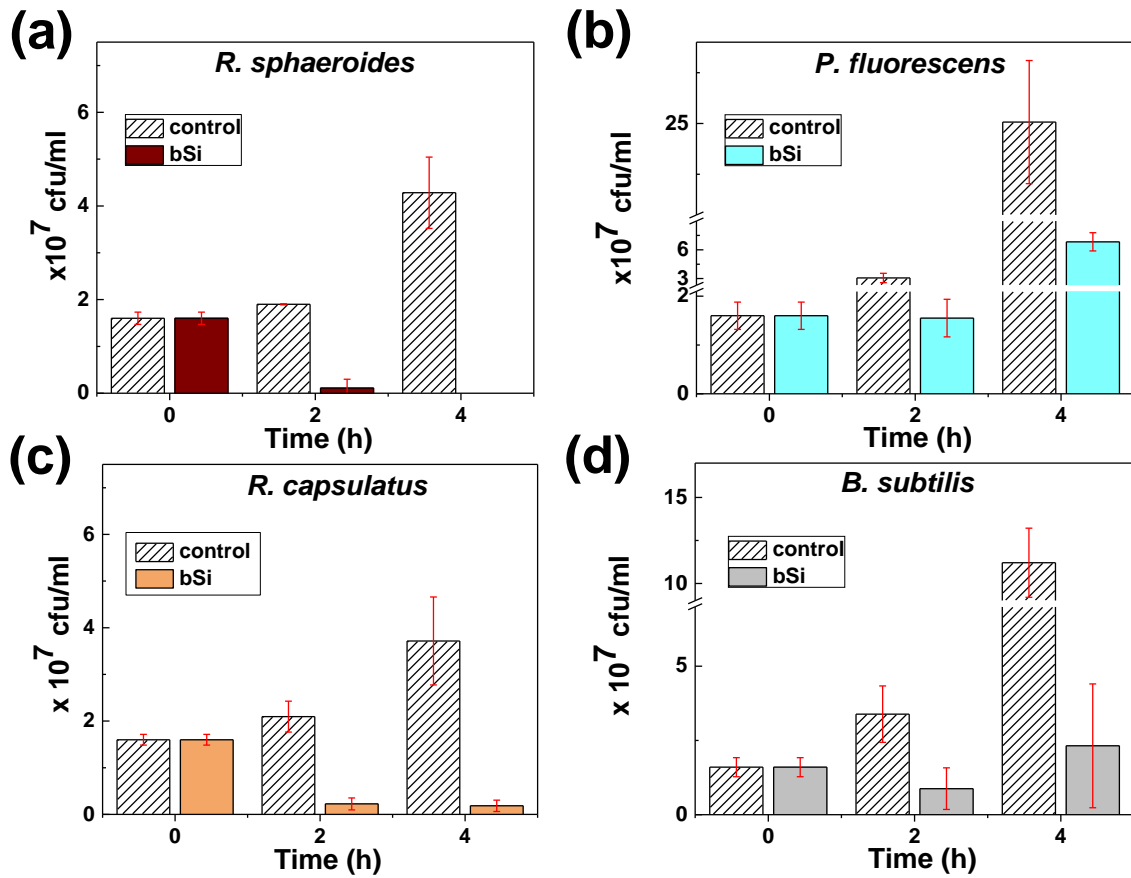


Fig. S9 The viability of (a) *R. sphaeroides*, (b) *P. fluorescens*, (c) *R. capsulatus*, and (d) *B. subtilis* on the bSi surface (3.6 μm). Colony forming units were measured by plating after exposure to etched (bSi) and smooth (control) surfaces in rich media for 2 or 4 h at room temperature. Cells clearly multiplied on the smooth surfaces whereas cells were killed or their growth inhibited on the nanostructured surfaces. The values are expressed as means \pm SD (n = 3 independent experiments).

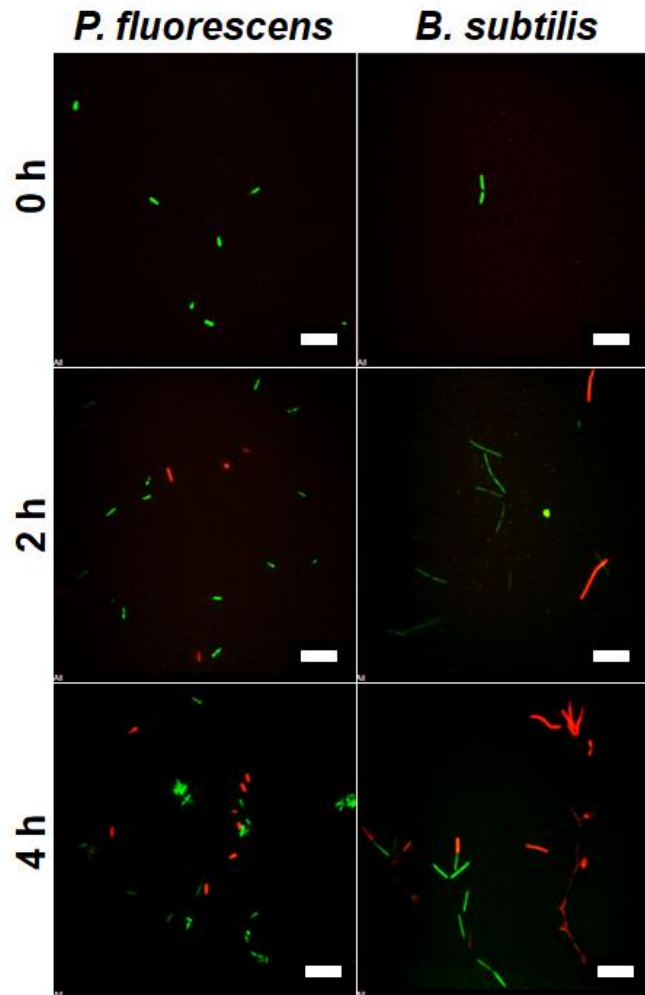


Fig. S10 Confocal microscopic images of *P. fluorescens* and *B. subtilis* attached to the surface of bSi (3.6 μm that corresponds sharp nanopillars) at 0, 2 and 4 h of incubation. Cells were stained with bacterial viability kit where green and red dyes label live and dead cells, respectively. Scale bar 10 μm .

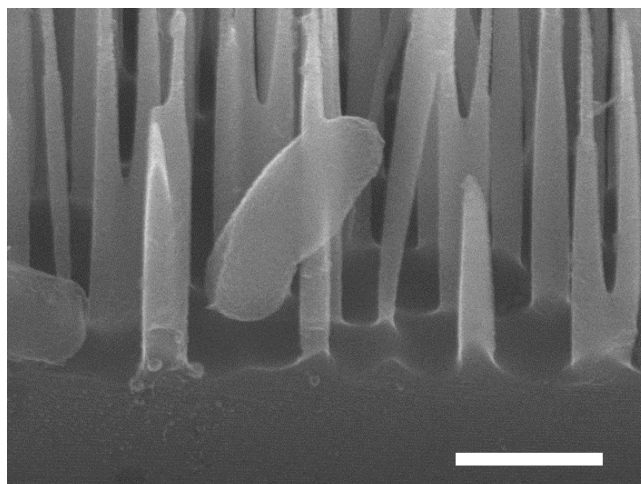


Fig. S11 SEM micrograph of *E. coli* with sharp nanopillar passing through. Scale bar 1 μm .

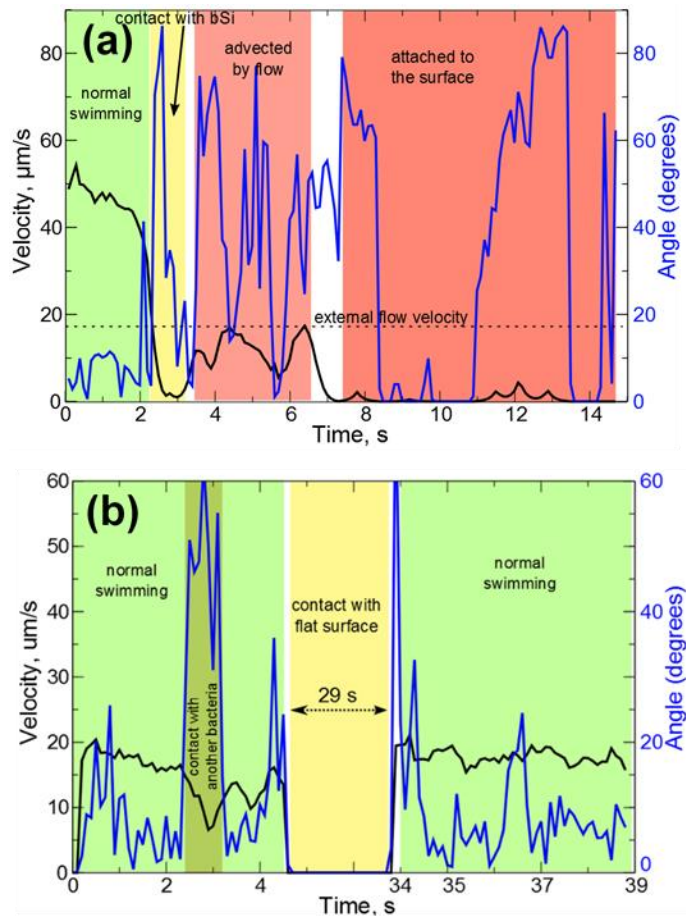


Fig. S12 The motility (velocity, black, and angle between cell orientation and velocity, blue) of single bacterial cells observed during initial interactions with either the benchmark bSi (a) or control (b) surfaces. In normal swimming periods (green), the bacteria move with high velocities and with relatively small angles between the cell's orientation and its velocity (<10 degrees). Motions can be briefly interrupted [yellow; 2.5-3.5 s, (a); 5-34 s, (b)] when the cell is likely in contact with the surface. Subsequently, a normal (b) or an irregular motion resumes [time interval 3.6-6.5 s, light peach coloring, (a)]. In the latter, the direction of the cell's motion is uncorrelated with its orientation. Moreover, its velocity becomes greatly reduced, resembling

that of the bulk flow. Although the cell is no longer attached to the surface, it likely lost its swimming ability and is just carried away by the external flow. Final permanent attachment [e.g, after 7.5 seconds in (a), dark orange] is characterized by zero velocity and random cell orientation. The cell interacting with bSi (a) was presumably killed when motility was terminated between 2.5-3.5 seconds. In contrast, the behavior and motility of the cell in contact with the control surface (b) was not altered by surface contact.

REFERENCES

- 1 V. Vadillo-Rodriguez and J. R. Dutcher, *Soft Matter*, 2009, **5**, 5012–5019.
- 2 M. E. Rhodes, *J. Gen. Microbiol.*, 1959, **21**, 221–263.
- 3 P. G. Adams and C. N. Hunter, *Biochim. Biophys. Acta - Bioenerg.*, 2012, **1817**, 1616–1627.
- 4 P. S. Raj, E. V. V Ramaprasad, S. Vaseef, C. Sasikala and C. V. Ramana, *Int. J. Syst. Evol. Microbiol.*, 2013, **63**, 181–186.
- 5 a O. Henriques, P. Glaser, P. J. Piggot and C. P. Moran, *Mol. Microbiol.*, 1998, **28**, 235–247.
- 6 S. B. Guttenplan, S. Shaw and D. B. Kearns, *Mol. Microbiol.*, 2013, **87**, 211–229.
- 7 V. Vadillo-Rodríguez and J. R. Dutcher, *Soft Matter*, 2011, **7**, 4101–4110.
- 8 H. H. Tuson, G. K. Auer, L. D. Renner, M. Hasebe, C. Tropini, M. Salick, W. C. Crone, A. Gopinathan, K. C. Huang and D. B. Weibel, 2012, **84**, 874–891.
- 9 J. Drelich, E. Chibowski, D. D. Meng and K. Terpilowski, *Soft Matter*, 2011, **7**, 9804.